Inorganica Chimica Acta, 144 (1988) 37–45

Interaction Between FeRu Bimetallic Carbonyl Clusters and Oxide Supports. V. $Fe_2Ru(CO)_{12}$ on Hydrated Silica

S. DOBOS, I. BÖSZÖRMÉNYI, J. MINK and L. GUCZI

Institute of Isotopes, Hungarian Academy of Sciences, H-1525 Budapest, P.O. Box 77, Hungary

(Received June 22, 1987)

Abstract

Thermal behaviour of the $Fe_2Ru(CO)_{12}$ bimetallic cluster on a SiO_2 support was studied by FT-IR spectroscopy. At room temperature most of the molecules quickly decompose into $Ru^0(CO)_2$, $Ru^{II}(CO)_2$ and $Ru^{III}(CO)_2$ species anchored to the silica surface, similarly to the behaviour of $Fe_2Ru(CO)_{12}$ on alumina. A smaller part (*ca.* 15%) of $Fe_2Ru(CO)_{12}$ is stable on the surface at room temperature in a distorted form. When heated in hydrogen and in vacuum a series of surface molecules has been identified: $H_2FeRu_3(CO)_{13}$, $H_4FeRu_3(CO)_{12}$, $H_4Ru_4(CO)_{12}$, and $HRu_3(CO)_{10}(OSi\leftarrow)$ anchored surface species. The ranges of thermal stability for the surface species have been given.

Introduction

In Part IV of this series it was shown, that $H_2FeRu_3(CO)_{13}$, on a silica surface, is rather stable, and the main reaction, when the adsorbed molecules were decomposed by heating in vacuum or in hydrogen, was a series of transformations into polynuclear molecular surface species and that the entity of the polynuclear metal frame was partly reserved [1]. Only a small amount of molecules had splitted into monometallic fragments, which supplied dicarbonyls, analogous to those found on alumina [2,3], anchored onto the silica surface. By this characteristic behaviour and the high stability, $H_2FeRu_3(CO)_{13}$ presents the most pronounced contrast to the cluster–support interactions experienced in the cases of bimetallic FeRu clusters adsorbed on alumina, where metal–metal bonds generally split producing anchored dicarbonyls as a unique type of stable surface species.

$Fe_2Ru(CO)_{12}$, represents the opposite case: its behaviour seems to be closer to that found on the very reactive alumina, than to that expected on silica.

Experimental

The experimental conditions were the same as in Part IV [1]. $Fe_2Ru(CO)_{12}$ was prepared by the method given in ref. 4. Infrared spectra of wafers pressed from the silica impregnated with the pentane solution of $Fe_2Ru(CO)_{12}$, and then dried in vacuum for 12 h to eliminate the solvent, were recorded in a heatable infrared cell in a hydrogen stream and in vacuum at temperatures ranging from 303 to 700 K. Baseline corrected double-beam spectra, where the sample completely decarbonylated at 700 K was used as reference, first and second derivatives of the spectra and difference spectra were computed, and in some cases a spectrum analysis was carried out by fitting Gaussians to the experimental spectra (for more information see also refs. 2 and 3).

Results and Discussion

Baseline corrected spectra of the system of $Fe_2Ru(CO)_{12}/SiO_2/H_2$ and $Fe_2Ru(CO)_{12}/SiO_2$/vacuum recorded at different temperatures, are shown in Fig. 1A and B, respectively, both figures completed with the spectrum of $Fe_2Ru(CO)_{12}$ in n-hexane solution, and also with the spectra recorded in hydrogen or in vacuum, at 303 K of $Fe_2Ru(CO)_{12}$ supported on hydrated alumina (spectra taken from Fig. 1A and B of ref. 2 and marked with Al_2O_3).

The first general impression is that the spectra contain the same main features as found in the case of alumina support. The similarity holds in hydrogen at already low temperatures, while in vacuum additional weak bands and/or shoulders are also observable up to 373 K. In reality these additional bands are present in vacuum up to 393 K, as can be seen in the second derivative representation of the spectra in Fig. 2B, and even in hydrogen they are seen up to 373 K (Fig. 2A). Remember, that the first and second derivatives of a spectrum emphasize the narrow components of a band system, however, they do not indicate the relatively broader ones, which means that the additional weak components of the band system should be narrower than those which in general govern the spectrum, and which are of the type of the bands recorded on alumina.

In Table I we have collected all the frequencies that had generally been identified using first of all

0020-1693/88/$3.50

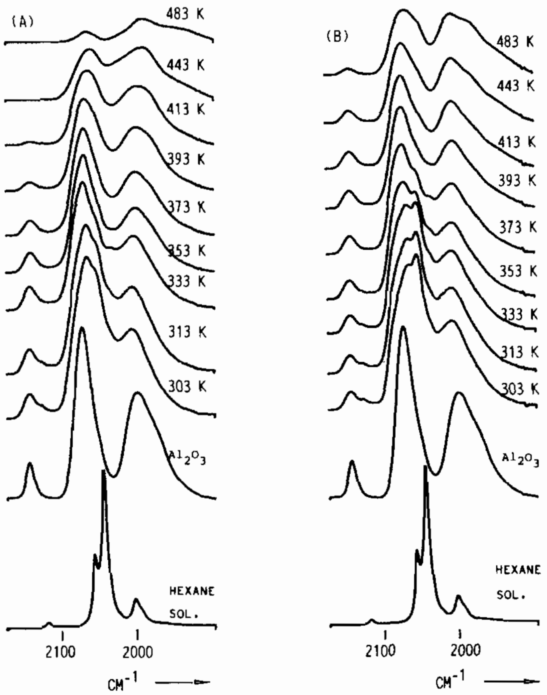

Fig. 1. Infrared spectra of the $Fe_2Ru(CO)_{12}/SiO_2$ system, recorded during decomposition in hydrogen (A), and in vacuum (B); spectrum of $Fe_2Ru(CO)_{12}$ in n-hexane solution (n-hexane) and analogous spectra of decomposition products on hydrated alumina recorded at 303 K (from ref. 2) (Al_2O_3).

second derivatives of Figs. 2A and B, (and, of course, using also the first derivatives, which, however, for the sake of brevity, we omitted here). The great number of frequencies located in this way are arranged into sets, that then could be assigned to surface molecules. These sets often contain several frequencies in coincidence. We emphasize that, when constructing the sets, we also made use of the difference spectra. The different kinds of surface molecules generally decomposed (or formed) in different temperature ranges and different spectra belonging to these ranges mainly represented the spectrum of the disappearing molecules helping us in performing assignments. The assignment, this time, turned out to be easier than it was in the case of $H_2FeRu_3(CO)_{13}$ in Part IV [1], because there was a lot of coincidences between the sets of frequencies, and, hence between the surface molecules derived from $Fe_2Ru(CO)_{12}$ and $H_2FeRu_3(CO)_{13}$. In Table I we also indicate the temperature range of the stability of the surface molecules.

Table I, however, does not show the relative amount of the different molecules on the surface. In order to estimate relative concentrations, we can make use of the analysis of some characteristic spectra, by fitting Gaussian components to the experimental data. In Fig. 3A–F the results of the analysis are seen, and in Table II the respective numerical data as well as intensities are given. It is obvious at first sight that the contribution of different di- or tricarbonyls of ruthenium to the overall intensity is dominant, even in vacuum and at the lowest temperature.

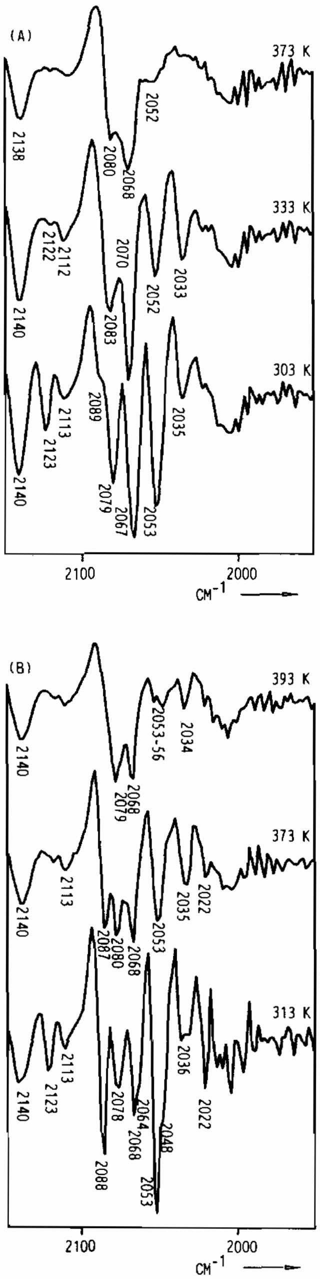

Fig. 2. Some characteristic second derivative spectra calculated from the spectra recorded during decomposition in hydrogen (A) and in vacuum (B).

A further basis that helps us to estimate relative amounts of surface molecules is both sets of difference spectra in Fig. 4A and B. Taking into account original spectra, derivatives, Gaussian analysis and

TABLE I. Infrared Spectral Data

Grouping of exp. IR bands	Frequency (cm^{-1})						Range of stability (K)		Assignment	Reference
							In vacuum	In hydrogen		
In solution	2118w	2058m	2046s	2005m	1994sh				$Fe_2Ru(CO)_{12}$	this work
Set I$^{a, b, c, d}$	2123w	2053m					303–413	303–353	$Fe_2Ru(CO)_{12}$	this work
In solution	2113vw	2085s	2074s	2041vs	2033m	1993w			$H_2FeRu_3(CO)_{13}$	1
Set II$^{b, d}$	2112	2089	2078	2052–2048	2034		303–393	303–313	$H_2FeRu_3(CO)_{13}$	this work
In solution	2085s	2070s	2054s	2031m	2012w	1998w			$H_4FeRu_3(CO)_{12}$	5
In solution	2083s	2068s	2056s	2033m	2026s	2008w			$H_2Ru_4(CO)_{13}$	8
Set III$^{b, d}$	2083	2070	2053	2033				333–373	$H_4FeRu_3(CO)_{12}$ $[H_2Ru_4(CO)_{13}]$	this work
In solution	2081s	2067vs	2030m	2024s	2009w				$H_4Ru_4(CO)_{12}$	5, 9
Set IV$^{b, c}$	2080	2068	2033	2022				303–373	$H_4Ru_4(CO)_{12}$	this work
	2112vw	2078s	2068s	2033vs	1995m,sh				$HRu_3(CO)_{10}(OSi\equiv)$	6
Set V$^{b, c}$	2112	2079	2068	2034			303–413		$HRu_3(CO)_{10}(OSi\equiv)$	this work
In solution	2063vs	2033s	2018m						$Ru_3(CO)_{12}$	this work
Set VI$^{b, d}$	2064	2036	2022				313–353		$Ru_3(CO)_{12}$	this work
Set VII$^{a, b, c, d}$	2140m	2074s					303–443	303–393	$Ru^{(III)}(CO)_2$	this work
Set VIII$^{a, c, d}$	2074vs	2009vs					303–483	303–413	$Ru^{(II)}(CO)_2$	this work
Set IX^{d}	2053s	1980s					303–483	303–483	$Ru^{(0)}(CO)_2$	this work

[a] Located in original spectra. [b] In derivative spectra. [c] In difference spectra. [d] From Gaussian analysis.

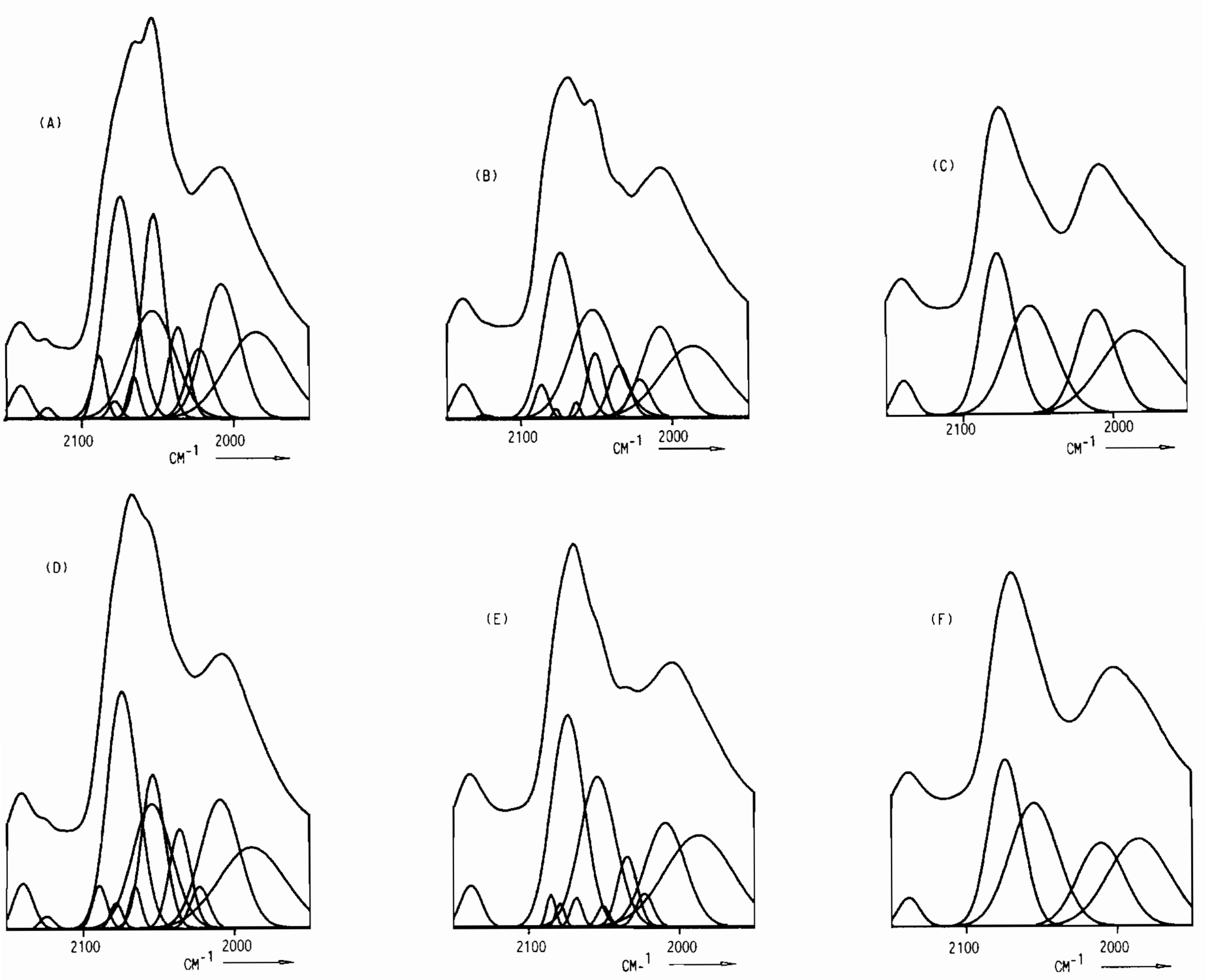

Fig. 3. Gaussian components calculated from the spectra recorded in the systems of $Fe_2Ru(CO)_{12}/SiO_2$/vacuum at the temperatures: (A) $T = 303$ K, (B) $T = 353$ K, (C) $T = 413$ K; and in the system of $Fe_2Ru(CO)_{12}/SiO_2/H_2$ at the temperatures: (D) $T = 303$ K, (E) $T = 333$ K and (F) $T = 373$ K.

difference spectra, we can locate the sets of spectral bands and the surface species the bands are assigned to, as follows below. It should be emphasized that molecular surface species have been found first of all in the system heated in vacuum. We also notice that the frequencies below and in Table I are generally values located not only from first and second derivative representation of the spectra and from difference spectra, but in the cases of broader bands, from Gaussian analysis, too.

Frequency Set I

The frequencies of 2123 and 2053 cm^{-1}, also located in the original spectra taken at lower temperatures, are to be assigned to adsorbed $Fe_2Ru(CO)_{12}$. In vacuum, at 303 K, its contribution to the total carbonyl stretching integrated intensity is about 15%, at 353 K about 5%, only, *i.e.* by heating, it gradually leaves the surface or rather decomposes. Transformation into other surface molecules is not as characteristic as it was in the case of $H_2FeRu_3(CO)_{13}$. Forming of new surface species during thermal treatment would produce positive peaks in the difference spectra in Fig. 4A and B, which, however, practically does not occur in the case of $Fe_2Ru(CO)_{12}$, except the broad positive band developing below 2000 cm^{-1} at higher temperatures. The lack of well distinguishable positive peaks in difference spectra, however, does not exclude the possibility of forming new species of very low concentration or even in traces, only. There are a few surface molecules discussed below, which supposedly develop by heating the sample, without producing detectable positive peaks in the difference spectra, because of their very low concentration.

In hydrogen the contribution of the bands of $Fe_2Ru(CO)_{12}$ to the total intensity is at the same level as in vacuum, but the decomposition already

TABLE II. Numerical Data of Gaussian Components of Spectra of Fig. 3A–F

Wavenumber ($\mathrm{cm^{-1}}$)	Gaussian width ($\mathrm{cm^{-1}}$)	Amplitude (abs. × 100)	Intensity (a.u.)	Ampl/GW	Assignment[a]
$\mathrm{Fe_2Ru(CO)_{12}/SiO_2}$/vacuum T = 303 K					
2140.6	6.4	6.3	101	1.0	$\mathrm{Ru^{(III)}(CO)_2}$
2123	3.8	2.2	20	0.6	$\mathrm{Fe_2Ru(CO)_{12}}$
2088.4	4.2	12	125	2.9	$\mathrm{H_2FeRu_3(CO)_{13}}$
2078	4.2	3.4	35	0.8	set II, V
2074	10	41.6	1042	4.2	$\mathrm{Ru^{(II)}(CO)_2}$, $\mathrm{Ru^{(III)}(CO)_2}$
2065.2	3.8	8	76	2.1	set V, VI
2052.4	7.4	38.2	708	5.2	set I, II
2053.4	15	20	751	1.3	$\mathrm{Ru^{(0)}(CO)_2}$
2036.2	6.6	17	281	2.6	set II, V, VI
2022	8.2	13	267	1.6	$\mathrm{Ru_3(CO)_{12}}$ $[\mathrm{Ru(CO)_2(OSi}\leqslant)_2]_n^*$
2007.2	12	25	751	2.1	$\mathrm{Ru^{(II)}(CO)_2}$
1984	20	16	802	0.8	$\mathrm{Ru^{(0)}(CO)_2}$
$\mathrm{Fe_2Ru(CO)_{12}/SiO_2}$/vacuum T = 353 K					
2140	6.6	6.5	107	1.0	$\mathrm{Ru^{(III)}(CO)_2}$
2126	5	0.8	10	0.2	$\mathrm{Fe_2Ru(CO)_{12}I}$
2087.8	4.4	6.4	70	1.5	$\mathrm{H_2FeRu_3(CO)_{13}}$
2078.4	2	2	10	1.0	set II, V
2074.8	11	31	854	2.8	$\mathrm{Ru^{(II)}(CO)_2}$; $\mathrm{Ru^{(III)}(CO)_2}$
2064.6	2.6	3.2	20	1.2	set V, VI
2053.4	15	20	751	1.3	$\mathrm{Ru^{(0)}(CO)_2}$
2051.8	5.6	12	168	2.1	set I, II
2035.8	6.8	9.6	168	1.4	set II, V, VI
2022	7	7	122	1.0	$\mathrm{Ru_3(CO)_{12}}$ $[\mathrm{Ru(CO)_2(OSi}\leqslant)_2]_n^*$
2007.8	12.4	16.8	522	1.4	$\mathrm{Ru^{(II)}(CO)_2}$
1986	21	13.2	694	0.6	$\mathrm{Ru^{(0)}(CO)_2}$
$\mathrm{Fe_2Ru(CO)_{12}/SiO_2}$/vacuum T = 413 K					
2139	6.8	6.5	110	1.0	$\mathrm{Ru^{(III)}(CO)_2}$
2074.8	11	30	827	2.7	$\mathrm{Ru^{(II)}(CO)_2}$, $\mathrm{Ru^{(III)}(CO)_2}$
2053.4	16	20	802	1.3	$\mathrm{Ru^{(0)}(CO)_2}$
2009	13	19	619	1.5	$\mathrm{Ru^{(II)}(CO)_2}$
1983	23	15	864	0.7	$\mathrm{Ru^{(0)}(CO)_2}$
$\mathrm{Fe_2Ru(CO)_{12}/SiO_2/H_2}$ T = 303 K					
2139.8	6.6	11.2	185	1.7	$\mathrm{Ru^{(III)}(CO)_2}$
2124.2	4.6	3.2	36	0.7	$\mathrm{Fe_2Ru(CO)_{12}}$
2089	4.8	10.6	127	2.2	set II, III, IV
2078	4	6.4	64	1.6	set III, IV
2073	10.2	57	1457	5.6	$\mathrm{Ru^{(II)}(CO)_2}$, $\mathrm{Ru^{(III)}(CO)_2}$
2065.4	3.8	10.4	99	2.7	set II, III, IV
2052.6	7.8	37	723	4.7	set I, II, VI
2053.4	13	30	977	2.3	$\mathrm{Ru^{(0)}(CO)_2}$
2035	7	24	421	3.4	set II, III, IV, VI
2022	6	10	150	1.7	$\mathrm{H_4Ru_4(CO)_{12}}$ $[\mathrm{Ru(CO)_2(OSi}\leqslant)_2]_n^*$
2008	13.2	31	1025	2.3	$\mathrm{Ru^{(II)}(CO)_2}$
1987	22	19.4	1069	0.9	$\mathrm{Ru^{(0)}(CO)_2}$

(continued)

TABLE II. *(continued)*

Wavenumber (cm^{-1})	Gaussian width (cm^{-1})	Amplitude (abs. × 100)	Intensity (a.u.)	Ampl/GW	Assignment[a]
$Fe_2Ru(CO)_{12}/SiO_2/H_2$ $T = 333$ K					
2138.6	7	10.3	180	1.5	$Ru^{(III)}(CO)_2$
2085	3	8	60	2.7	set II, $\underline{\text{III}}$, $\underline{\text{IV}}$
2079	3	6	45	1.6	set III, IV
2073.6	11	51	1406	4.6	$Ru^{(II)}(CO)_2$, $Ru^{(III)}(CO)_2$
2068	3.8	7	66	1.8	set II, III, IV, (V), VI
2049.8	4	5	50	1.6	set $\underline{\text{I}}$, II, VI
2053.4	12	36	1082	3.0	$Ru^{(0)}(CO)_2$
2033.6	6.4	17	272	2.7	set II, $\underline{\text{III}}$, $\underline{\text{IV}}$
2022	5.6	8	112	1.4	$H_4Ru_4(CO)_{12}$ $[Ru(CO)_2(OSi\lessdot)_2]_n$*
2008	13.4	25	839	1.9	$Ru^{(II)}(CO)_2$
1985.6	22.6	22	1246	1.0	$Ru^{(0)}(CO)_2$
$Fe_2Ru(CO)_{12}/SiO_2/H_2$ $T = 373$ K					
2138.2	7.2	7	126	1.0	$Ru^{(III)}(CO)_2$
2073.4	11	40	1102	3.6	$Ru^{(II)}(CO)_2$, $Ru^{(III)}(CO)_2$
2054.4	16	29.6	1187	1.6	$Ru^{(0)}(CO)_2$
2009.2	15.6	20	782	1.3	$Ru^{(II)}(CO)_2$
1984	20.4	21	1073	1.0	$Ru^{(0)}(CO)_2$

[a] See text for starred items.

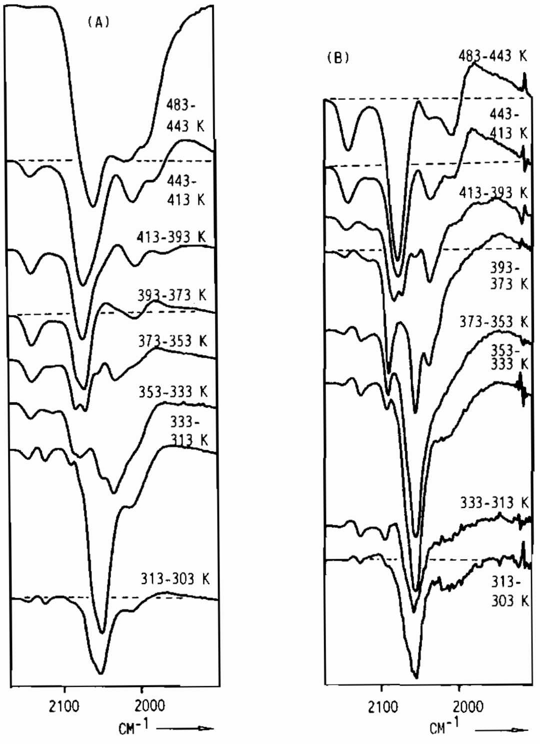

Fig. 4. Difference spectra calculated from the spectra of Fig. 1A (A) and B (B).

occurs between 313–333 K, as also seen in the respective spectrum in Fig. 4A.

The shape of the bands of adsorbed $Fe_2Ru(CO)_{12}$ is more distorted than it was in the case of $H_2FeRu_3(CO)_{13}$; for instance the components at the frequencies 2058 and 2046 cm^{-1} well separated in solution of non-polar solvents, at adsorbed molecules are not resolved. This fact suggests that the molecules of $Fe_2Ru(CO)_{12}$ are significantly perturbed on the surface.

Frequency Set II

The frequencies of set II (2112, 2089, 2078, 2048 and 2034 cm^{-1}), although their contribution to the total carbonyl intensity cannot be higher than 5%, are very easy to assign to weakly bonded and slightly perturbed $H_2FeRu_3(CO)_{13}$ surface molecules (frequencies in solution: 2113vw, 2085s, 2074s, 2041vs, 2033m, and 1993w cm^{-1}). On the other hand, its concentration on the surface, in comparison to that of $Fe_2Ru(CO)_{12}$ is surprisingly high, and it shows, that in the surface layer the mobility of the molecules during or immediately after impregnation (before thermal treatment) must be very easy, and surface molecular reactions are possible, where traces of surface water are favorable to formation of hydrido complexes, first of all that of $H_2FeRu_3(CO)_{13}$. $H_2FeRu_3(CO)_{13}$ being the main molecular product of

$\mathrm{Fe_2Ru(CO)_{12}}$–surface interaction, one expects that the pathway of forming further surface molecules might be similar to that experienced on the $\mathrm{H_2FeRu_3(CO)_{13}/SiO_2/H_2}$ or $\mathrm{H_2FeRu_3(CO)_{13}/SiO_2}$/vacuum systems [1].

Frequency Set III

In accordance with the above expectation the next surface molecule (with the frequencies 2083, 2070 and 2053 $\mathrm{cm^{-1}}$), that has been detected, only however on the sample heated in hydrogen stream, is $\mathrm{H_4FeRu_3(CO)_{12}}$ (frequencies in solution 2085s, 2070s, 2054s, 2031m, 2012w and 1998w $\mathrm{cm^{-1}}$ [5]). It should be only present in traces, but in a rather wide range of stability from room temperature up to 373 K. $\mathrm{H_4FeRu_3(CO)_{12}}$ can be derived from $\mathrm{H_2FeRu_3(CO)_{13}}$ by the reaction $\mathrm{H_2FeRu_3(CO)_{13} + H_2 = H_4FeRu_3(CO)_{12} + CO}$, that is, its formation supposes the presence of $\mathrm{H_2}$. As shown in Part IV, this frequency set may indicate the presence of $\mathrm{H_2Ru_4(CO)_{13}}$, as a byproduct surface molecule, too [1].

Frequency Set IV

The frequencies of 2080, 2068, 2033 and 2022 $\mathrm{cm^{-1}}$, only measured in hydrogen, can be assigned to $\mathrm{H_4Ru_4(CO)_{12}}$ surface molecule (in solution 2081s, 2067vs, 2030m, 2024 and 2009w $\mathrm{cm^{-1}}$ [5,9]). In vacuum, it very possibly does not occur [1], because $\mathrm{H_2}$ is favorable for the formation of $\mathrm{H_4Ru_4(CO)_{12}}$. The difference spectrum 373–353 K in Fig. 4A shows a considerable amount of $\mathrm{H_4Ru_4(CO)_{12}}$ leaving the surface or decomposing.

Frequency Set V

The frequencies 2112, 2079, 2068 and 2034 $\mathrm{cm^{-1}}$ are to be assigned to the surface species $\mathrm{HRu_3(CO)_{10}(OSi{\lessdot})}$, grafted to the surface, as also found on silica supported $\mathrm{Ru_3(CO)_{12}}$ [6]. As shown in Part IV, its presence in hydrogen is less probable than in vacuum, and we have consequently found that its range of stability is rather wide in vacuum. In vacuum $\mathrm{HRu_3(CO)_{10}(OSi{\lessdot})}$ practically decomposes in one step between 393–413 K (see Fig. 4B). We don't believe that formation of $\mathrm{HRu_3(CO)_{10}(OSi{\lessdot})}$ starts from $\mathrm{H_2FeRu_3(CO)_{13}}$, because in the systems of $\mathrm{H_2FeRu_3(CO)_{13}/SiO_2}$ we have found practically no (or in traces, only) $\mathrm{HRu_3(CO)_{10}(OSi{\lessdot})}$. It is most probable that in the system of $\mathrm{Fe_2Ru(CO)_{12}/SiO_2}$/vacuum $\mathrm{HRu_3(CO)_{10}(OSi{\lessdot})}$ is directly formed from $\mathrm{Fe_2Ru(CO)_{12}}$ through the cleavage of metal–metal bonds, and by a rearranging of Ru atoms into $\mathrm{Ru_3}$ frames.

Frequency Set VI

Set VI (2064, 2036 and 2022 $\mathrm{cm^{-1}}$) is assigned to $\mathrm{Ru_3(CO)_{12}}$ (in solution 2063vs, 2033s and 2018m $\mathrm{cm^{-1}}$), which may be regarded as an intermediate to several surface molecules, first of all to that of $\mathrm{HRu_3(CO)_{10}(OSi{\lessdot})}$, as it can be derived from both $\mathrm{Fe_2Ru(CO)_{12}}$ [3] and $\mathrm{H_2FeRu_3(CO)_{13}}$ [1,3]. It has only been detected in vacuum.

It should be noticed, that the band at 2022 $\mathrm{cm^{-1}}$ has a very high intensity (see Table II) and, therefore, it probably belongs to a surface species of $\mathrm{[Ru^{II}(CO)_2(OSi{\lessdot})_2]_n}$, as shown by Zanderighi *et al.* in the case $\mathrm{Ru_3(CO)_{12}}$ adsorbed on silica [6].

Frequency Set VII

The pair of bands 2053s–1986s (set VII) we assigned to the surface dicarbonyl $\mathrm{Ru^{(0)}(CO)_2}$, anchored to the surface, as in the case of $\mathrm{H_2FeRu_3(CO)_{13}}$. This type of dicarbonyl has also been found on alumina support [2]. Its contribution to the total carbonyl stretching intensity is between 30–50% in vacuum (in hydrogen somewhat higher), consequently its concentration should also be very high. The integrated intensity of both bands of the pair are practically equal, that means that the angle between the two carbonyls is 90°. On this basis we suggest an octahedral symmetry for the $\mathrm{Ru^{(0)}(CO)_2}$ species.

Frequency Sets VIII–IX

Continuing to draw parallelism between dicarbonyls on silica surface and those on alumina, the pairs of bands 2074–2009 $\mathrm{cm^{-1}}$ (set VIII), and 2139–2074 $\mathrm{cm^{-1}}$ (set IX) should be assigned to $\mathrm{Ru^{(II)}(CO)_2}$ and $\mathrm{Ru^{(III)}(CO)_2}$, respectively [2,3]. However, an assignment of set IX to a dicarbonyl of triply oxidized ruthenium raises some doubts. The coincidence of the second band of set IX with that of the first one of set VIII (both 2074 $\mathrm{cm^{-1}}$), makes an estimation of the contribution of both sets to the intensity of the band at 2074 $\mathrm{cm^{-1}}$ difficult, and hence, the calculation of the ratios of the intensities of the bands in the sets VIII and IX. From the difference spectra 443–413 K and 483–443 K (experiment in vacuum, Fig. 4B), where the difference is mainly the (negative) spectrum of set IX (*i.e.*, in these ranges of temperatures the dominant event is the decomposition of the surface species the set IX belongs to), we can estimate a ratio for the bands of set IX of about 1:3. Supposing that $\mathrm{Ru^{(III)}(CO)_2}$ dicarbonyl is responsible for the set IX, the angle between the two C–O bonds calculated from the intensity ratio 1:3 is 97°. Zanderighi *et al.* assigned these two bands measured on silica supported $\mathrm{Ru_3(CO)_{12}}$ to $\mathrm{Ru^{(II)}(CO)_3}$ [6]. For a $\mathrm{Ru(CO)_3}$ group the angles between the CO bonds calculated from the above intensity ratio would be 51° which value seems unrealistic. Therefore we believe that set IX is to be assigned to the dicarbonyl $\mathrm{Ru^{(III)}(CO)_2}$ of octahedral or tetrahedral conformation rather than to the tricarbonyl $\mathrm{Ru^{(II)}(CO)_3}$. The contribution of the intensity of set IX to the total intensity varies between 10–15%.

If we substract the intensity of the band at 2139 cm^{-1} times 3 from the intensity of the band at 2074, we get the approximative intensity for the band at 2074 cm^{-1} belonging to set VIII. Further, the ratio of the intensities of the bands of set VIII suggest an angle near 90° in the dicarbonyl of $Ru^{(II)}(CO)_2$, the surface species set VIII is to be assigned to. Although the precision of the calculation of the above angle is rather unsatisfactory, it suggests an octahedral rather than a tetrahedral configuration. The contribution of the intensity of set VIII to the total intensity of carbonyls is very high: about 35% in both vacuum and hydrogen.

Bridging Carbonyls

In Fig. 1A and B we have not shown the frequency range of bridging carbonyls (1900–1800 cm^{-1}), because the bands of the bridging carbonylic system are very weak on the scale of Fig. 1A and B, and they do not practically rise above the background. Even in the solution in non-polar solvent of n-hexane, the ratio between the integrated intensity of terminal CO bands and those of bridging ones is 26:1 [7]. Supported on silica, where at the beginning of thermal decomposition the concentration of $Fe_2Ru(CO)_{12}$ is very low (*ca.* 15%), very weak and hardly detectable bridging carbonylic bands are expected. Although this is the expectation, we have managed to get a spectrum recorded at room temperature on the sample treated in hydrogen. The spectrum on expanded scale (with numerical results of Gaussian analysis) is seen in Fig. 5. For comparison, in the same Fig. 5, we also show the positions of the bands of bridging carbonyls of $Fe_2Ru(CO)_{12}$ in n-hexane solution [7]. It is very surprising, that the dominant features of the band system, the pair of bands (B,B′) at 1876 and 1856 cm^{-1}, are at higher frequencies than the highest ones experienced in solution, namely that measured in n-hexane: 1865 and 1834 cm^{-1}; although in solution, with increasing polarity of the solvent, a shift to lower frequencies takes place [7]. Furthermore, the difference between the frequencies of the $Fe_2Ru(CO)_{12}$ bonded to the silica surface is 20 cm^{-1}, in contrast to that in solution of 31 cm^{-1}. This means that:

(i) The structure of bridges in the surface molecule $Fe_2Ru(CO)_{12}$ should essentially differ from that in solution. This fact should be considered in connection with our opinion expressed when discussing the frequency set I: that the molecule is significantly distorted in comparison to the free molecule or to the molecule of $H_2FeRu_3(CO)_{13}$ which is bonded on the silica surface by weak physisorption or weak hydrogen bonding [1].

(ii) The higher frequencies exclude the possibility that the molecules of $Fe_2Ru(CO)_{12}$ are bonded to the silica surface with hydrogen bonding between the bridging CO and one or more silanol groups.

(iii) The higher frequencies refer to considerably shorter C–O distances in the bridging structure of the surface molecule, which surprisingly indicate asymmetric or rather incipient bridges.

(iv) The smaller difference between the frequency pairs suggests a weaker coupling between both CO oscillators, which is in accordance with the conclusion of (iii).

The angle of the two C–O bonds of the bridging pair of carbonyls estimated from their intensity ratio is 97°.

The bridging band system also contains a second, weaker pair of bands (A,A′), with frequencies of 1864 and 1840 cm^{-1}, close to those found in n-hexane solution, and with an angle of C–O bonds of 121°, somewhat larger than that in n-hexane of 114.4° (recalculated from intensity data given in ref. 7). This second double bridging carbonylic structure seems to belong to molecules less perturbed, and hence a smaller part of the $Fe_2Ru(CO)_{12}$ molecules (*ca.* 1/6) should be bonded to the surface by weak physisorption.

	CM^{-1}	WIDTH	AMPL.	INT.
A	1840	5.4	0.36	4.9
B	1856	7.2	1.10	19.9
A′	1864	3.6	0.17	1.5
B′	1876	7.8	0.80	15.6

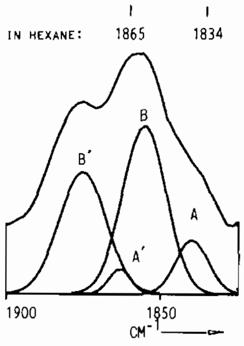

Fig. 5. Expanded IR spectrum of bridging carbonyls of the system of $Fe_2Ru(CO)_{12}/SiO_2/H_2$ at $T = 303$ K, with Gaussian components.

Conclusions

(a) In the series of bimetallic clusters of $Fe_2Ru(CO)_{12}$, $FeRu_2(CO)_{12}$ and $H_2FeRu_3(CO)_{13}$, the molecule of $Fe_2Ru(CO)_{12}$ is the least stable on hydrated silica. After impregnation while keeping the sample in vacuum for 12 h at room temperature, in the majority of the molecules (70–80%) the metal–metal frame collapses forming supposedly monometallic, that is highly dispersed, ruthenium carbonyls of the type of $Ru^{(0)}(CO)_2$, $Ru^{(II)}(CO)_2$ and $Ru^{(III)}(CO)_2$.

(b) By the low stability, the behaviour of $Fe_2Ru(CO)_{12}$ on hydrated silica is – to a certain extent – similar to that on alumina.

(c) The main product (about 35%) of the interaction of $Fe_2Ru(CO)_{12}$ with silica is the dicarbonyl of $Ru^{(0)}(CO)_2$ anchored onto the surface. The angle of 90° between the two C–O bonds suggests an octahedral configuration for this species. $Ru^{(0)}(CO)_2$ is very stable, it decomposes at temperatures $T > 483$ K in both hydrogen and vacuum.

(d) The concentration of the next monometallic anchored surface species of $Ru^{(II)}(CO)_2$ is also very high (about 30%). The angle between the C–O bonds of about 90° also suggests an octahedral configuration. $Ru^{(II)}(CO)_2$ is also stable, it decomposes at temperatures $T > 413$ K in hydrogen and $T > 483$ K in vacuum.

(e) The next monometallic anchored surface species is that of $Ru^{(III)}(CO)_2$ (concentration about 10–15%). The angle of 97° between the C–O bonds indicates an octahedral or tetrahedral configuration. $Ru^{(III)}(CO)_2$ decomposes at somewhat lower temperatures of $T > 393$ K in hydrogen and $T > 443$ K in vacuum.

(f) During the interaction between $Fe_2Ru(CO)_{12}$ and silica – in contrast to its behaviour on hydrated alumina – a series of molecular surface species also occurs.

(g) Original molecules of $Fe_2Ru(CO)_{12}$ found on the surface at room temperature in a concentration of about 15% may be regarded as the main molecular surface species. Its molecules are rather perturbed, that is manifested in the distorted and unresolved spectra of the terminal CO stretching modes, and in the unusual structure of the bridging carbonyls. $Fe_2Ru(CO)_{12}$ decomposes in the temperature range of 303–413 K in vacuum and 303–353 K in hydrogen.

(h) $H_2FeRu_3(CO)_{13}$ (*ca.* 5%) is considered as the first and main product of the surface molecular reactions of $Fe_2Ru(CO)_{12}$ after impregnation, and in developing further surface molecules $H_2FeRu_3(CO)_{13}$ should be regarded as a starting compound. It is detectable on the surface in the temperature range of 303–393 K in vacuum and 303–313 K in hydrogen.

(i) In hydrogen the pathway of thermal reactions is similar to that of $H_2FeRu_3(CO)_{13}$ adsorbed on silica [1], supporting the conclusion of (h). In vacuum $H_2FeRu_3(CO)_{13}$ practically does not take part in the surface reactions, which behaviour is also similar to that of the system of $H_2FeRu_3(CO)_{13}/SiO_2$/vacuum [1].

(j) In accordance with (i) the next surface molecule detected in traces on the sample heated in hydrogen, is that of $H_4FeRu_3(CO)_{12}$ that can be derived from $H_2FeRu_3(CO)_{13}$ by the reaction: $H_2FeRu_3(CO)_{13} + H_2 = H_4FeRu_3(CO)_{12} + CO$. Formation of $H_2Ru_4(CO)_{13}$, at this stage of the surface reactions, is also thought to be a byproduct [1]. Stability range: 333–373 K.

(k) The next surface molecule detected in traces on the sample heated in hydrogen is $H_4Ru_4(CO)_{12}$, stable in the temperature range of 303–373 K. It practically decomposes in one step between $T =$ 353–373 K.

(l) In vacuum the pathway of thermal surface reactions is different. $Ru_3(CO)_{12}$ as a surface intermediate molecule derived from $Fe_2Ru(CO)_{12}$ [3] is detected in traces in the temperature range of 313–353 K.

(m) From $Ru_3(CO)_{12}$ the next species developed in vacuum and grafted to the surface, namely that of $HRu_3(CO)_{10}(OSi\leftarrow)$ (detected in traces in the temperature range of 303–413 K), can be derived. It practically decomposes in one step between $T =$ 393–413 K.

References

1 S. Dobos, I. Böszörményi, J. Mink and L. Guczi, *Inorg. Chim. Acta, 134,* 203 (1987).
2 S. Dobos, I. Böszörményi, J. Mink and L. Guczi, *Inorg. Chim. Acta, 120,* 135 (1986).
3 S. Dobos, I. Böszörményi, J. Mink and L. Guczi, *Inorg. Chim. Acta, 120,* 145 (1986).
4 D. B. W. Yawney and F. G. A. Stone, *J. Chem. Soc. A,* 502 (1969).
5 S. A. R. Knox, J. W. Koepke, M. A. Andrews and H. D. Kaesz, *J. Am. Chem. Soc., 97,* 3942 (1975).
6 G. M. Zanderighi, C. Dossi, R. Ugo, R. Psaro, A. Theolier, A. Choplin, L. D'Ornelas and J. M. Basset, *J. Organomet. Chem., 296,* 127 (1985).
7 (a) S. Dobos, S. Nunziante-Cesaro and M. Maltese, *Inorg. Chim. Acta, 113,* 167 (1986); (b) S. Dobos, A. Beck, S. Nunziante-Cesaro and M. Barbeschi, *Inorg. Chim. Acta, 130,* 65 (1987).
8 B. F. G. Johnson, R. D. Johnstone, J. Lewis and B. H. Robinson, *J. Chem. Soc. A,* 2856 (1968).
9 G. L. Geoffroy and W. L. Gladfelter, *J. Am. Chem. Soc., 99,* 7565 (1977).